In situ observation of the spherulite deformation in polybutene-1 (Modification I)

E. WEYNANT, J. M. HAUDIN
Centre de Mise en Forme des Matériaux, Ecole des Mines de Paris, Sophia Antipolis, 06560 Valbonne, France

C . G'SELL
Laboratoire de Physique du Solide, Ecole des Mines de Nancy, Parc de Saurupt, 54042 Nancy, France

Stress–strain behaviour under uniaxial tension was determined for polybutene-1 specimens with various spherulite sizes and degrees of crystallinity. Samples with large spherulites and a high crystallinity level exhibited a very specific behaviour, characterized by a higher elastic modulus, a remarkably homogeneous deformation (absence of necking), a stress whitening phenomenon and a brittle intraspherulitic rupture. The deformation mechanisms have been analysed by means of *in situ* microscopic observations. It was shown that interlamellar separation, which occurred first in the equatorial regions perpendicular to the tensile axis, is mainly responsible for the observed phenomena.

1. Introduction

One of the most important aspects in the study of the mechanical behaviour of semi-crystalline polymers is the observation of the morphological changes induced by the deformation. Thus, the deformation of spherulites, which is the basic morphology for melt crystallized polymers, has been investigated several times by direct microscopic observations [1–10]. The experiments have been performed by optical or electron microscopy either on strained cast films or on microtomed sections from polymeric samples deformed in the bulk.

Previous work, which essentially concerned polyethylene and polypropylene, has shown that the plastic deformation of these polymers was in general inhomogeneous on a microscopic as well as on a macroscopic scale. Within each spherulite, it was shown that the deformation of the radial crystalline lamellae depended on their orientation with respect to the draw direction. The resulting deformation of each spherulite is not affine and it was then shown that the models taking into account an affine deformation [11, 12] only give a first approximation of the actual deformation within the spherulite. The response of spherulites to a deformation appeared to result from a number of mechanisms including slip, tilt and twinning of the crystalline lamellae. It was proved in many cases to be highly recoverable [3–5, 9]. Besides this complexity, which is inherent in all spherulitic polymers, the plastic deformation of polyethylene and polypropylene is affected by the early occurrence of a necking process. This plastic instability, which occurs even at very small strain rates, made the quantitative study of the spherulite deformation rather difficult, since true strain and stress vary at a given time along the investigated deforming film.

The present work was devoted to the deformation and rupture of spherulites in polybutene-1 (Modification I) specimens which exhibit no plastic instability while deforming plastically. Particular attention was paid to the quantitative correlation between spherulite morphology and macroscopic mechanical behaviour. The evolution within individual large size spherulites will be reported during uniaxial tensile tests thanks to the use of *in situ* characterization techniques.

2. Experimental procedure

2.1. Crystalline structure of the material

Isotactic polybutene-1 is a linear semi-crystalline polyolefin with the following formulation

$$\left[\begin{array}{c} - CH_2 - CH - \\ | \\ C_2H_5 \end{array} \right]n \; .$$
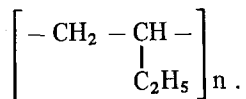
When this material solidifies from the melt, the chains crystallize in a spherulitic morphology; it will be seen that a very large range of spherulite sizes can easily be obtained with suitable crystallization temperatures.

With respect to other polyolefins, polybutene-1 exhibits an original polymorphic behaviour. Several crystalline modifications were reported in the literature [13–16]. The most important ones are called I and II, respectively. The tetragonal Modification II, obtained by crystallization from the melt, is unstable and transforms into the stable Modification I, which is described as hexagonal or rhombohedral. The transformation occurs spontaneously within a few days [17, 18] and can be considerably accelerated by pressure or stress [6, 13, 19–21].

In this paper only the deformation of polybutene spherulites, in which the crystalline phase is completely transformed into Modification I will be considered.

2.2. Sample preparation

An experimental grade of sample was mainly used, supplied through the courtesy of CdF Chimie (grade 0.5, molecular weight $M_w = 550\,000$, density 0.910). Experiments were also performed with a commercial material (Hüls Vestolen BT 8000: grade 0.1, $M_w = 1\,225\,000$, density 0.914). No major differences were observed in the crystalline morphologies of both polymers nor in their mechanical properties.

Films were obtained by pressing the molten polymer at $170°$ C between two glass slides and then crystallizing it. Two types of films were used in this work: (1) films with homogeneous spherulite size were prepared in several ways (isothermal crystallization, quenching, controlled cooling) in order to obtain specimens with various spherulite diameters; (2) films with a few large spherulites embedded in a matrix of very small spherulites were obtained by uncompleted high temperature crystallization followed by quenching.

Just after the crystallization process, the specimens were in the unstable Modification II. After ageing for several days at room temperature, the films were fully transformed into the stable Modification I.

2.3. Tensile tests

The stress–strain behaviour of the material was determined at room temperature with an Instron tensile testing machine. Samples were cut out of films prepared as described above.

For the *in situ* observation of the spherulite deformation, a special tensile device was designed and mounted on the stage of a transmission optical microscope (Fig. 1). As shown in Fig. 2, this small tensile machine has two grips (G and G') to which a strip of film (S) can be attached. Their movements are guided by two ball sliders (BS and BS'). The right hand grip can be displaced by means of a micrometric screw (M); the left hand grip is attached to a force transducer (FT). The apparatus thus ensures a simultaneous measurement of the specimen elongation (by the micrometer screw vernier) and of the applied load (by the force transducer electronic conditioner).

2.4. Other techniques

Further information was obtained by additional techniques. The melting point and the degree of crystallinity of the samples were determined by differential scanning calorimetry (Perkin Elmer DSC 2 calorimeter). The spherulite diameter was measured by the small angle light scattering (SALS) technique [22], when it was not possible to measure this parameter directly by optical microscopy, e.g. in the case of small spherulites. Finally, the orientation of the crystalline phase was examined by wide angle X-ray scattering, using the flat film camera technique (filtered $CuK\alpha$ radiation).

3. Results

3.1. Macroscopic plastic behaviour as a function of the crystalline morphology

In order to determine their macroscopic stress–strain behaviour, specimens with five types of microstructure were tested in tension with an Instron machine. They were obtained by crystallization from the melt by five different techniques:

Sample 1: crystallization on quenching in liquid nitrogen.

Sample 2: crystallization on quenching in iced water.
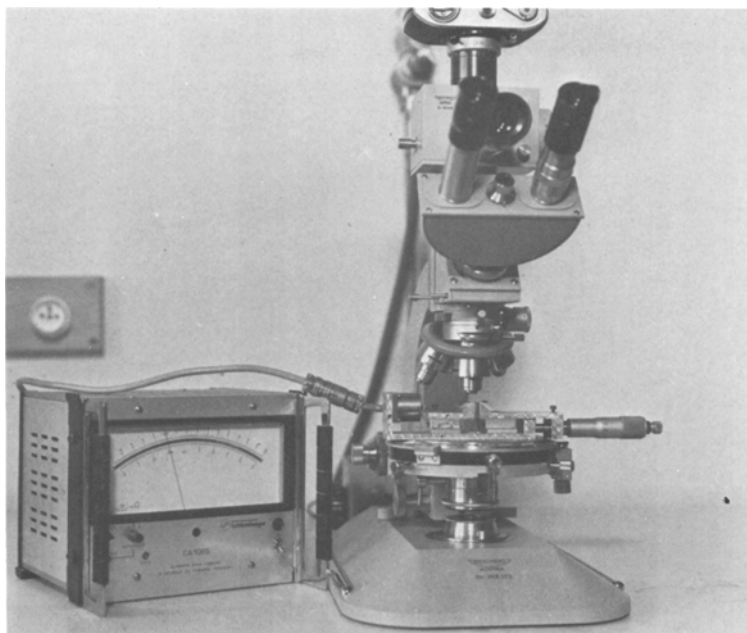
Sample 3: crystallization in air at $25°$ C.

Figure 1 Overall view of the tensile machine on the stage of the polarizing microscope.

Sample 4: crystallization in air at 75° C.

Sample 5: crystallization during controlled cooling at 0.2° C min^{-1} in a regulated hot stage. (Spherulites appeared at 102° C and crystallization was completed at 80° C).

The characteristic size of the spherulitic morphology of these specimens is given in Fig. 3 from optical microscopic observations or small angle light scattering experiments. It is seen that the various crystallization procedures led to different spherulite diameters ranging from 1 μm (specimens quenched in liquid nitrogen) to more than 1 mm (slowly cooled specimens).

Samples 1, 2 and 3 exhibit a four-lobe SALS pattern, which is characteristic of a spherulite morphology [22]. For Sample 1, the absence of extinction at the centre of the diagram indicates that, in this specimen, the small spherulites are not completely developed [23]. For Samples 4 and 5, with much larger spherulites, the SALS technique does not provide any valuable information, due to the very small size of the lobes, which are additionally masked by a diffusion halo.

In addition to this geometrical characterization of the spherulites, a complementary study was performed by differential scanning calorimetry in order to determine the degree of crystallinity of the samples. The results, also shown in Fig. 3, show that the weight fraction of crystallized polymer gradually increases from 43% in Sample 1 to 76% in Sample 5.
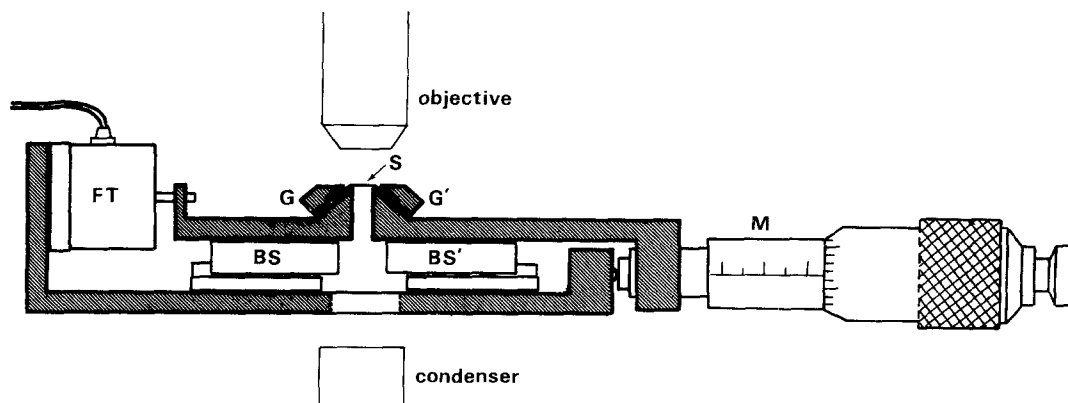
The tensile specimens were cut out of the films

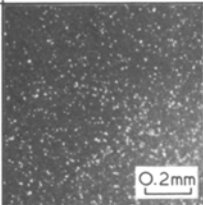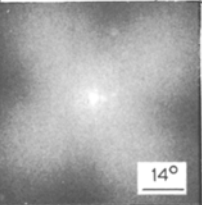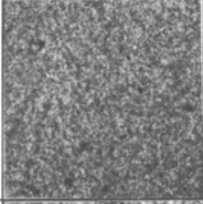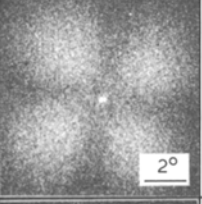*Figure 2* Detailed diagram of the miniaturized tensile machine.

2679
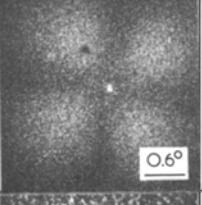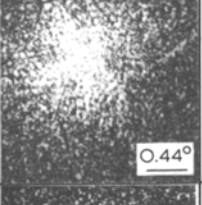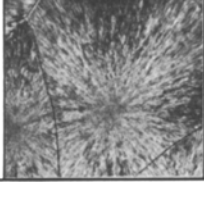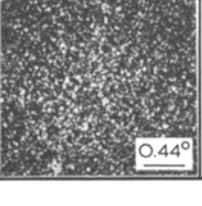
n°	spherulite size		diameter	cristallinity by D.S.C.		
	optical micrography (crossed polarizers)	small angle light scattering		T_m (°C) ΔH_f (cal g⁻¹)		wt % crystal.
1	0.2mm	14°	1 µm	108 13		43
2		2°	15	115 17.1		57
3		0.6°	60	119 17.5		58
4		0.44°	400	125 19.2		68
5		0.44°	1100	126.5 22.9		76

Figure 3 Characterization of the five specimens tested in tension on the Instron machine. The molten polymer was pressed at 170° C between two glass slides and crystallized by the following techniques: Sample 1 — quenching in liquid nitrogen; Sample 2 — quenching in iced water; Sample 3 — crystallization in air at 25° C; Sample 4 — crystallization in air at 75° C; Sample 5 — controlled cooling at 0.2° C min⁻¹. For each specimen, the spherulite diameter, the melting temperature T_m, the enthalpy of fusion per unit mass ΔH_f and the weight fraction crystallinity have been reported.

prepared by these five procedures. Their initial dimensions were carefully measured. Typical values of the calibrated length, width and thickness were $L_0 = 16$ mm, $l_0 = 3.5$ mm and $t_0 = 0.3$ mm, respectively. Tensile tests were performed with a constant elongation rate of $\dot{L} = 5$ mm min⁻¹ (constant nominal rate $\dot{\epsilon}_N \simeq 5 \times 10^{-3}$ sec⁻¹). Nominal stress—strain curves were deduced from the experimental load—elongation charts and are shown in Fig. 4. It appears that the mechanical

behaviour of the specimens varied considerably with their crystalline structure. For small and partially amorphous spherulites, the material was soft and ductile, whereas it was hard and brittle in the case of large and well crystallized spherulites. For all the samples, the deformation was at least partly recoverable. For instance in the case of the ductile Sample 1, the total nominal strain (elastic + plastic) just before rupture was $\epsilon_N = 1.57$. After rupture, a permanent plastic strain
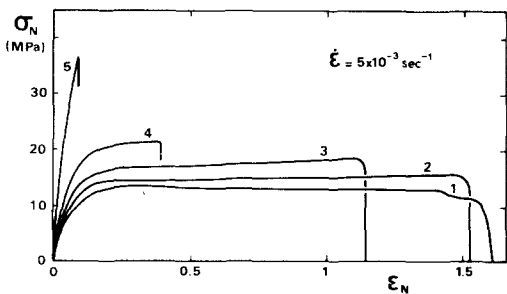
Figure 4 Nominal stress versus nominal strain curves of the specimens.

$\epsilon_{pl} = 1.04$ was measured, hence an elastic recovery $\epsilon_{el} = 0.53$.

Another striking feature of this tensile behaviour of polybutene-1 specimens is the remarkable homogeneity of the deformation. In Samples 3, 4 and 5, the material is not affected by any plastic instability, in contrast with polyethylene and polypropylene [24, 25]. Samples 1 and 2 exhibit some evidence of necking (note the small yield drop in the nominal stress–strain curves). Necking is very discrete in Sample 2, and a little more pronounced in Sample 1.

Thanks to the homogeneity of the plastic deformation of polybutene, its true stress–strain $\sigma(\epsilon)$ behaviour can be derived easily from the nominal curves $\sigma_N(\epsilon_N)$ by using the expressions $\sigma = \sigma_N(1 + \epsilon_N)$ and $\epsilon = \ln(1 + \epsilon_N)$. (These equations are invalid for polyethylene and polypropylene for which it was shown [26] that more sophisticated experiments are required to obtain the $\sigma(\epsilon)$ curves.) The results are displayed in Fig. 5 and show that polybutene can be characterized by a rubber-like elastic behaviour with a low initial modulus and a gradual yielding followed by progressive strain hardening.

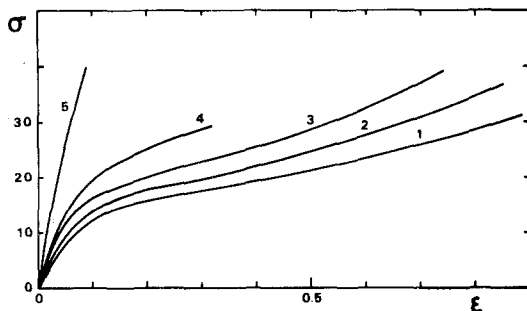Comparison of the five curves indicates that an increase in crystallinity and spherulite diameter

Figure 5 True stress versus true strain curves deduced from the data of Fig. 4.

produces a reinforcement of the material and its embrittlement. The absence or small importance of necking is simply due to the fact that the slope $d\sigma/d\epsilon$ of the $\sigma(\epsilon)$ curves never fulfills the modified Considere criterion $d\sigma/d\epsilon < \sigma$, except in a very short interval in the knee of the curves for Samples 1 and 2.

The visual observation of the specimens during tensile testing shows a white turbidity for Samples 4 and 5 with large spherulites and a high crystalline fraction while the ones with smaller spherulites and lower crystallinity remain nearly translucent. This whitening, which could be at first sight taken as a simple crazing phenomenon, appeared gradually from the very beginning of the tests and could be shown to be nearly completely reversible up to true strains of about 0.1. Sample 5 thus returned to its initial state of translucence after rupture, while Sample 4 retained a considerable amount of whitening.

The rupture mechanism of the specimens was itself very dependent on the microstructural features. For samples with small and less crystalline spherulites, specimens failed in a very ductile way through a gradual tearing from an initial defect (bubble) or at the grip level. Conversely, the specimens with large spherulites and a high crystalline fraction exhibited a very sudden and brittle fracture.

3.2. Characterization of the microstructure of the specimens after rupture

The microstructure of broken samples, whose stress–strain curves were analysed above, were examined.

Wide angle X-ray scattering photographs of Samples 3 to 5 were observed to be quite similar to those of the undeformed samples. A typical example of such a pattern is shown in Fig. 6a. It consists of continuous diffraction rings characteristic of Modification I (the strongest observed ones being 110, 300 and 220 + 211), without any visible intensity reinforcement. It can be deduced that no pronounced crystalline orientation remained after rupture in these specimens, even in the vicinity of the rupture region. Conversely in Samples 1 and 2, which were subjected to larger strains, the diffraction patterns (Figs 6b and c) exhibit local intensity reinforcements which indicate some orientation of the chain axis towards the drawing direction.

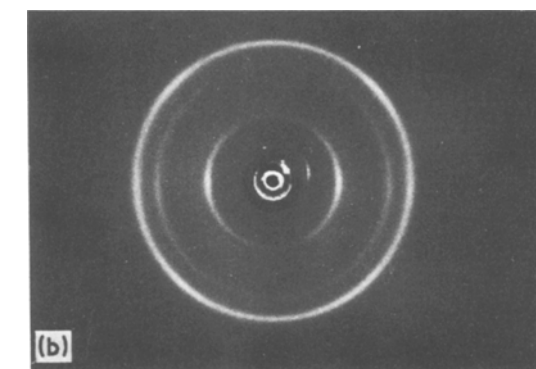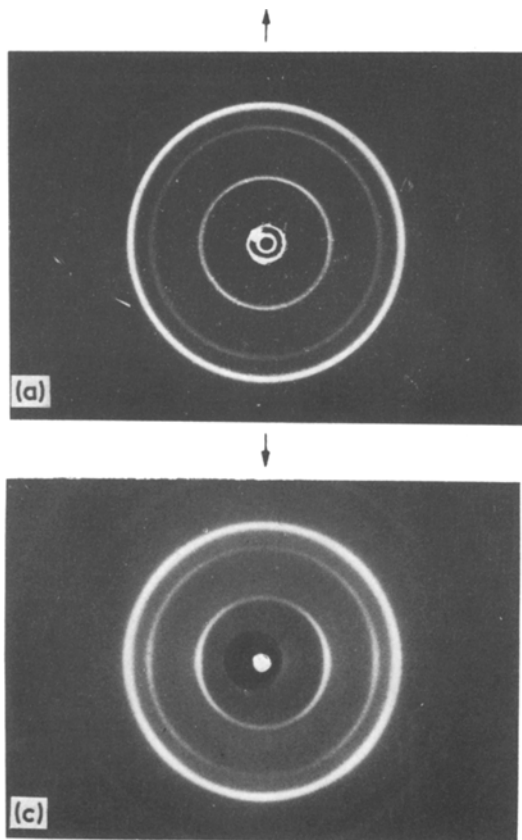The broken specimens were also analysed by

Figure 6 Wide angle X-ray diffraction patterns of tensile tested specimens. (a) Sample 4 (crystallization in air at 75° C), (b) Sample 2 (crystallization during quenching in iced water) and (c) Sample 1 (crystallization during quenching in liquid nitrogen).

small angle light scattering. The patterns obtained with Samples 1, 2 and 3 are displayed in Fig. 7. Compared with the corresponding ones before deformation (Fig. 3), they are of the four-lobe type with an elongation of the lobes perpendicular to the tensile axis, according to the model proposed by Samuels [27]. It is seen that the elongation of the lobes in the patterns of Samples 1 and 2 is much more pronounced than in the pattern of Sample 3. These results show that, during the stretching of these specimens, the fine spherulites keep their identity by plastic elongation parallel to the tension axis. For the last two samples, with much larger spherulites, (Samples 4 and 5), it can be seen that the SALS technique does not provide any valuable information.

Fortunately, in the case of large spherulites, optical microscopy gives direct evidence of their evolution. Fig. 8 shows this aspect of the morphology in Sample 4 after rupture. It is characterized by slightly deformed spherulites; in each of them a dark equatorial band perpendicular to the tensile axis can be observed. The existence of these bands in transmission optical microscopy

corresponds to the visual observations of whitening in reflected light.

From these results, it appears that the microstructure of plastically deformed samples remains essentially spherulitic, because of the moderate strains reached in these experiments. No transformation from a spherulitic into a fibrillar texture was observed, as was previously noted with more severe types of sollicitation, such as compression [28].

3.3. *In situ* observations of the deformation of individual spherulites

The aim of the following section is to analyse by fine scale microscopic observation, the morphological evolution occurring within large spherulites during plastic deformation. This characterization will first be made on a specimen with homogeneous spherulite morphology and will then be studied more closely in the case of a sample with few large spherulites, embedded in a microspherulitic matrix.

A polybutene film, $40 \mu m$ thick (Sample 6) was completely crystallized in a regulated hot stage at 80° C and then slowly cooled to room temperature. A strip, 1.1 mm wide, was cut out of the film and attached to the miniaturized tensile machine described in Section 2.3 with a calibrated length of 3.2 mm.

Fig. 9a shows the initial spherulitic morphology with a distribution of diameter centered around a mean value of $160 \mu m$. The sample was gradually
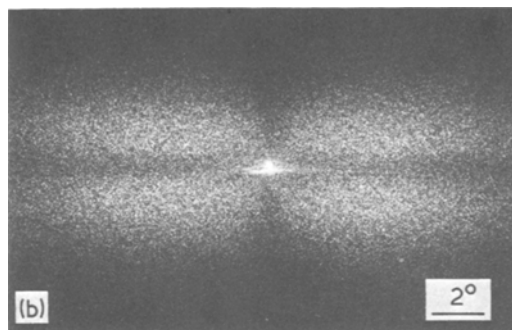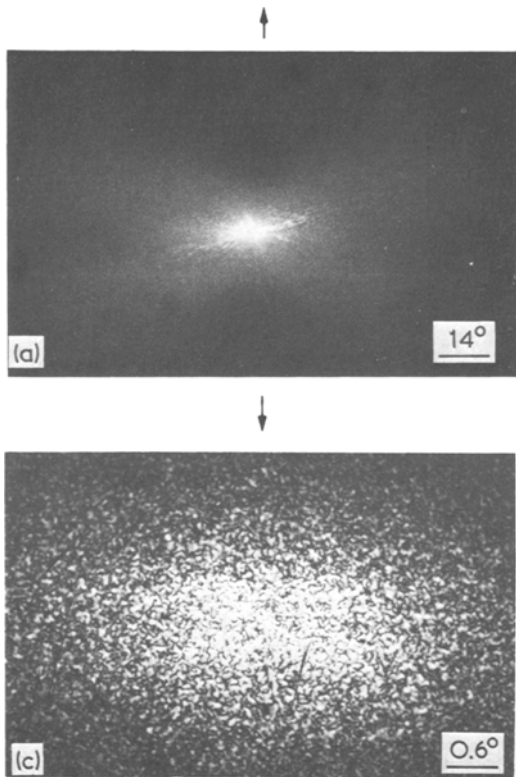
strained by operating the micrometric screw. The photograph in Fig. 9b was obtained for a true strain of $\epsilon = 0.13$ and under a true stress of $\sigma = 11$ MPa. It shows, that, between crossed polarizers respectively parallel and perpendicular to the tensile axis, the development of a dark and broad band within each spherulite. This band lies in the equatorial region of the spherulites, perpendicular to the tensile direction and then superimposes on one pair of arms of the initial maltese crosses. On further stretching the specimen (Fig. 9c, $\epsilon = 0.21$, $\sigma = 14$ MPa), it is seen that these dark bands extended laterally.

Although thin strips, such as the one described above, give far better microscopic observation conditions than the thicker ones used in macroscopic tests, they are unfortunately affected by early brittle ruptures due to geometric imperfections. The observation of the dark band could not be continued up to larger strains. In order to avoid this experimental difficulty, an extensive study of this phenomenon was made on large spherulites in a ductile microspherulitic matrix, which can accomodate much larger strains.

The photograph in Fig. 10a shows the initial configuration of a single spherulite observed in a

film, 95 μm thick, quenched during slow cooling (Sample 7). It has a nearly perfect disc shape and extends over the whole thickness of the film. Its diameter is 370 μm. The concentric external layer corresponds to the curvature of the growth front during the crystallization process. The spherulite is completely surrounded by very fine spherulites which cannot be resolved at this magnification by optical microscopy. As above, the film was gradually strained in the small tensile testing machine. For various stages of deformation, microscopic observations were systematically performed in three different ways: (1) between crossed polarizers respectively parallel and perpendicular to the tensile axis; (2) between crossed polarizers, having their polarization axes at ± 45° to the tensile axis; (3) with unpolarized light.

At each step, the longitudinal and transverse true strains, ϵ_L and ϵ_T, were determined from
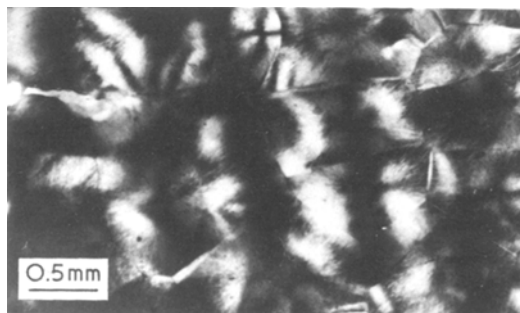

Figure 8 Microscopic characterization of Sample 4 (crystallized in air at 75° C) after rupture.
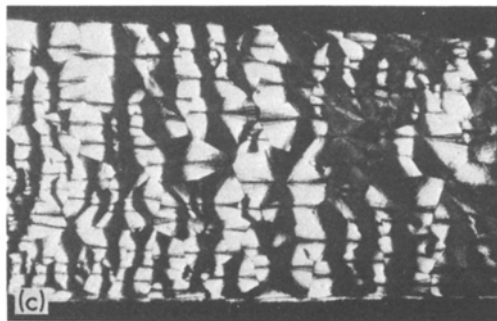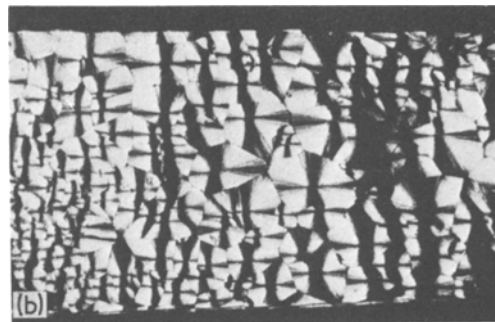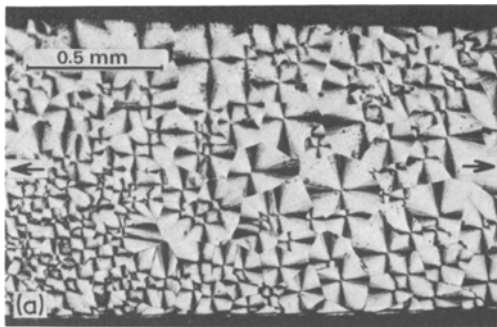
2683

Figure 9 *In situ* observation using crossed polarizers of the evolution of the spherulites in a sample whose crystallization was completed at 80° C. The true longitudinal strains and stresses are (a) $\epsilon = 0$ $\sigma = 0$ MPa, (b) $\epsilon = 0.13$ $\sigma = 11$ MPa and (c) $\epsilon = 0.21$ $\sigma = 14$ MPa.

measurements of the longitudinal and transverse dimensions of the spherulite in the micrographs.

It can be seen that deformation begins at the centre of the spherulite. At early stages of drawing ($\epsilon_L = 0.01$), a small dark spot is clearly visible on the micrograph taken with unpolarized light (Fig. 10b). It rapidly transforms into a small dark band perpendicular to the tensile axis (Fig. 10c). This band extends radially until it reaches the spherulite boundary (Fig. 10d, $\epsilon_L = 0.08$, $\epsilon_T = -0.05$), and becomes broader with increasing strain (Fig. 10d to f). Then, the spherulite elongates more and more in the drawing direction, and the equatorial dark band can now be described as two opposite symmetrical sectors (Fig. 10g to i). For the most important strains ($\epsilon_L > 0.85$), the equatorial region appears to be less dark between crossed polarizers parallel and perpendicular to the tensile axis. Moreover, the arms of the maltese cross perpendicular to the tensile axis again become slightly visible (Fig. 10h and i). For such strains, a dark line can be observed, between crossed polarizers at $\pm 45°$, in the polar regions parallel to the stretching direction (Fig. 10i, $\epsilon_L = 0.95$, $\epsilon_T = -0.38$). With increasing strain, this line gradually becomes coloured according to the different interference colours. This isochromatic line is not visible when the polarizers are parallel or perpendicular to the

tensile axis, because it is masked by the maltese cross. After rupture, which occurred in another region of the film, the dark band is still present (Fig. 10j); an important elastic recovery can be observed, the permanent strains after rupture being $\epsilon_L = 0.74$ and $\epsilon_T = -0.30$.

The evolution of the dark equatorial band for large strains has been shown by a complementary study performed on other films, crystallized by the same procedure as Sample 7. Fig. 11a shows, for a longitudinal strain $\epsilon_L \sim 0.6$, three large spherulites which had an initial diameter of about 300 μm (Sample 8). It can be seen that the dark region extends over almost the whole surface of the spherulites. However, in the largest one, some evidence of whitening can already be observed at its centre. The micrograph of Fig. 11b has been taken for $\epsilon_L \sim 0.8$, i.e. for a strain of the same order of magnitude as in Fig. 10h. In each spherulite the dark region has regressed. For much larger strains and just before rupture (Fig. 11c, $\epsilon_L \sim 1.1$), it has completely disappeared, and a deformed maltese cross is now visible within the spherulites.

Eventually, the rupture region in broken samples was observed, either with homogeneous texture (Sample 6) or with large spherulites in a microspherulitic matrix (Sample 7). In the first case, Fig. 12 gives evidence of the intraspherulitic character of the rupture: the break-line has clearly progressed along a zig-zag path within successive spherulites, passing near their centre and always following a spherulite radius. In the second case Fig. 13 also shows the brittleness of the large spherulites with respect to the small ones. It
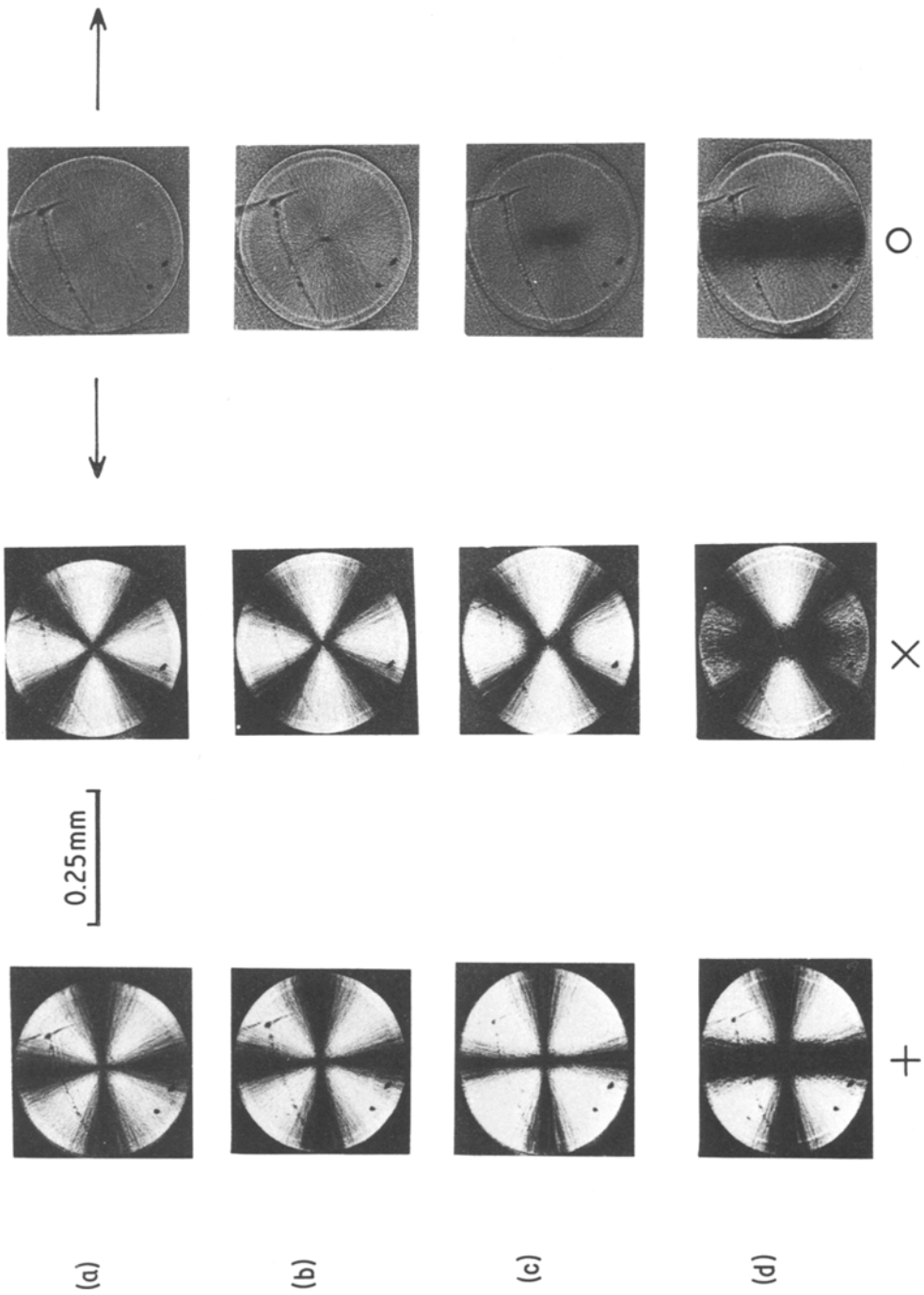
Figure 10 *In situ* observation of the evolution of a single spherulite embedded in a microspherulitic matrix (for each step of strain, the spherulite is observed with (+) crossed polarizers parallel and perpendicular to the tensile axis, (×) crossed polarizers at 45° to the tensile axis and (○) unpolarized light). The true longitudinal and transversal strains are (a) $\epsilon_L = 0$, $\epsilon_T = 0$, (b) $\epsilon_L = 0.01$, $\epsilon_T > -0.01$, (c) $\epsilon_L = 0.06$, $\epsilon_T = -0.02$, (d) $\epsilon_L = 0.08$, $\epsilon_T = -0.05$, (e) $\epsilon_L = 0.12$, $\epsilon_T = -0.06$, (f) $\epsilon_L = 0.41$, $\epsilon_T = -0.1$, (g) $\epsilon_L = 0.53$, $\epsilon_T = -0.2$, (h) $\epsilon_L = 0.85$, $\epsilon_T = -0.32$, (i) $\epsilon_L = 0.95$, $\epsilon_T = -0.38$ and (j) after rupture, $\epsilon_L = 0.74$, $\epsilon_T = -0.30$.
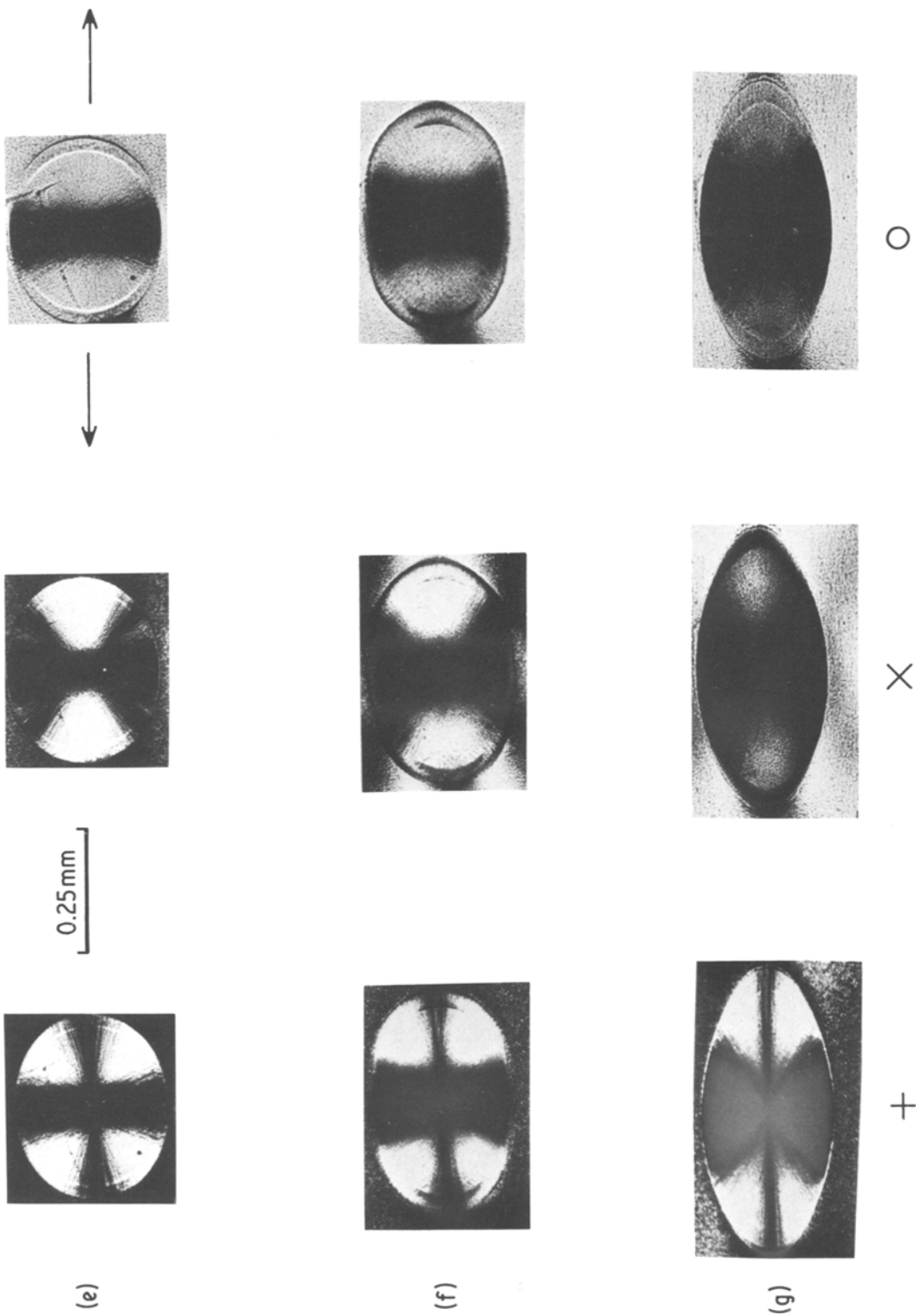
2685

0.25 mm

(e)

(f)

(g)

○

✕

+

Figure 10 Continued.
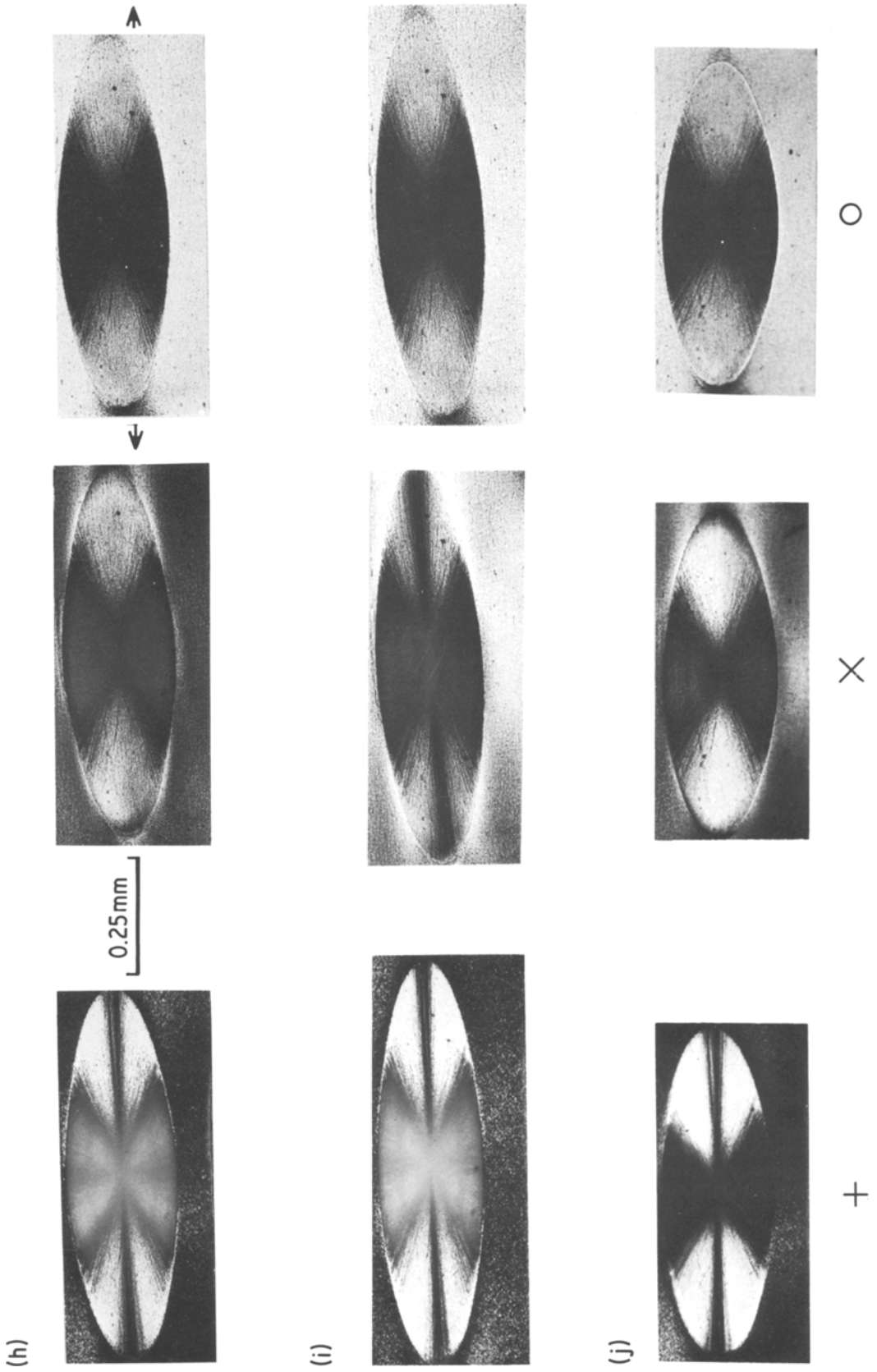
0.25 mm

(h)

(i)

(j)

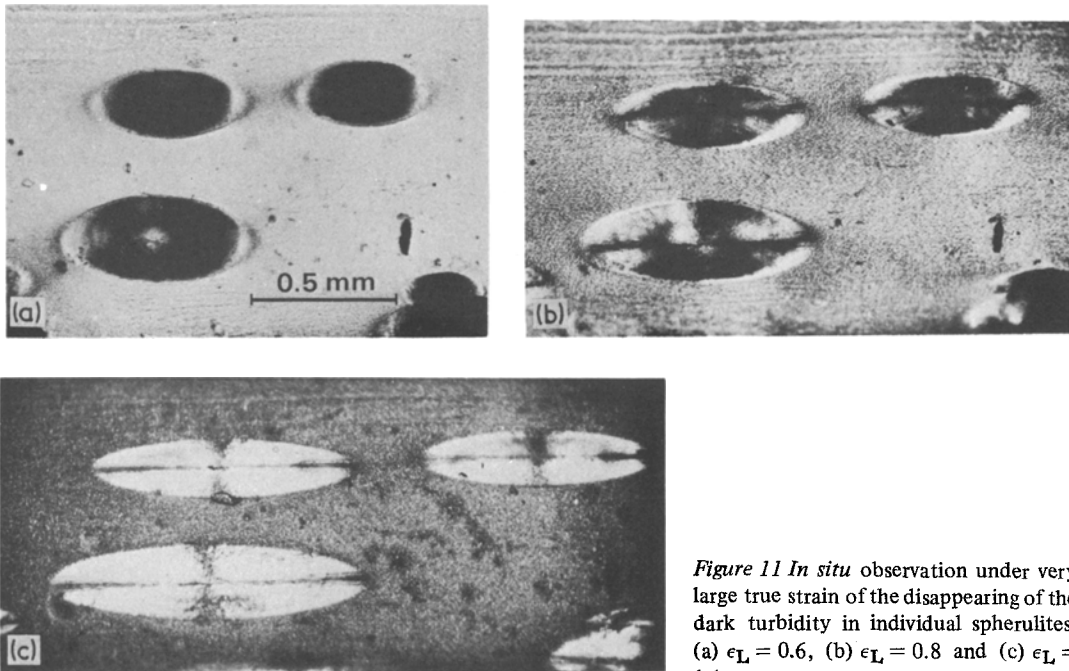O

×

+

Figure 10 Continued.

2687

Figure 11 *In situ* observation under very large true strain of the disappearing of the dark turbidity in individual spherulites. (a) $\epsilon_L = 0.6$, (b) $\epsilon_L = 0.8$ and (c) $\epsilon_L = 1.1$.

always appears that rupture occurs preferentially in places of the film where a larger number of big spherulites are found and it can be seen that the break-line passes through them.

4. Discussion
4.1. The dark band phenomenon
All the experimental results reported in the previous section show that polybutene-1 specimens with large spherulites exhibit a very specific behaviour with respect to those with smaller spherulites during straining. It was observed by transmission optical microscopy that deformation within these large spherulites was inhomogeneous and that the most important morphological feature was the occurrence and development of a dark equatorial band. The existence of this band in the spherulites corresponds to the whitening of the strained samples, detected by visual observation. In this section, it is mainly the origin of this dark band that will be discussed.

This dark band appears for small strains in the equatorial region perpendicular to the tensile axis, firstly at the core of the spherulite. This means that this region, particularly the centre of the spherulite, is subjected to higher strains and stresses. This result is in agreement with previous experimental observations [3, 6] and was also predicted by the theoretical calculations of Wang [29]. In his model, Wang considered an individual

spherical spherulite of polyethylene embedded in a homogeneous matrix having the properties of the polymer. His analysis, based on linear elasticity, reveals very high stress and strain concentrations around the origin of the spherulite. His results also indicate that the strain in the stretching direction is much higher in the equatorial than in the polar region. This strain being normal to the lamellar crystals in the equatorial region, tends to separate them. Furthermore, the existence of compressive strains along the radius, measured in our experiments ($\epsilon_T < 0$) and also predicted in the theoretical analysis of Wang [29], is likely to induce some lamellar bending.

From the above considerations, it can be inferred, that the first stage of deformation in the equatorial region perpendicular to the tensile axis consists of interlamellar separation and lamellar bending.

This mechanism induces density lowering or void formation in the amorphous interlamellar region. Thus the density fluctuation between amorphous and crystalline layers is considerably increased, and an important light scattering phenomenon arises from this fluctuation, as previously analysed by Debye and Bueche [30]. This scattering phenomenon is responsible for the milky turbidity observed by visual examination during tensile tests, and for the dark band observed by optical microscopy. In the latter case, it had
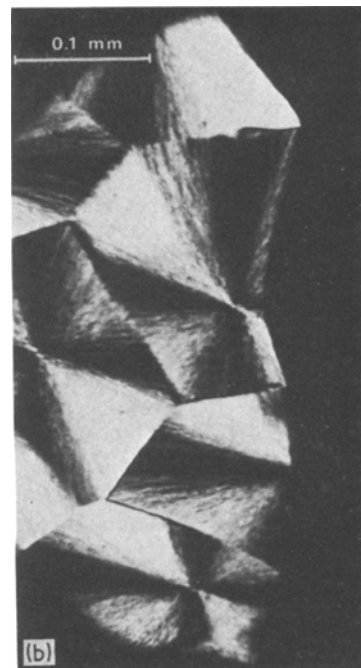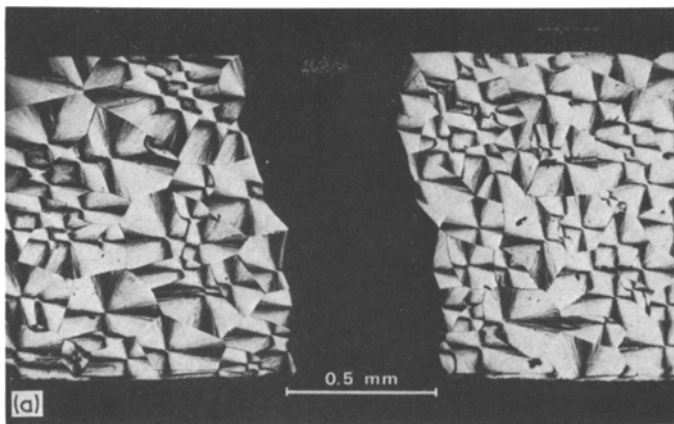
Figure 12 Fracture of the sample whose deformation was examined *in situ* in Fig. 9. (a) Overall view and (b) detailed aspect of the intraspherulitic fracture.

already been shown that the dark band was not due to a polarization effect, because it was observed with different positions of the crossed polarizers, and even with unpolarized light. Moreover, the hypothesis of a scattering effect has been proved by a simple additional experiment. Upon immersing the stretched films for a sufficient time in a liquid with a refractive index of 1.51, i.e. close to the index of amorphous polymer, the turbidity completely disappeared, the films again being translucent. At the same time, the dark band was no longer observed by optical microscopy. The liquid penetrates into the void region and decreases the density fluctuation between the crystalline lamellar and the interlamellar regions.

This deformation mechanism (separation and bending of lamellae) can be compared with the deformation of some fibres and films, which have been called "hard elastic" in the literature [31−33]. Their microstructure consists of stacks of orientated lamellae connected by tie links, their normal being parallel to the tensile axis. While stretching the specimen, the lamellar network splays apart between tie links, with consequent interlamellar void generation. In our polybutene-1 specimens, tie molecules were certainly present between lamellae because of the rather high molecular weights of the polymers used. Also, the above mechanism concerns untwisted lamellae, or, at least, lamellae with a relatively low degree of twisting. Polybutene-1 specimens with large spherulites have been obtained by high temperature crystallization. In such conditions, the degree of twisting is lowered. Furthermore, even in low

temperature crystallization, twisting never seems to be very important, because no banded spherulites were observed.

4.2. Irreversible plastic deformation

It has been shown that, with increasing strain, the dark band reaches diagonal regions where the spherulite radii make an angle θ lower than $90°$ with the tensile axis. In such regions, lamellae are not only subjected to a normal strain, which tends to separate them, but also to shear strains [29]. These strains induce a rotation of lamellae towards the stretching direction, so that the initial circular shape is converted into an ellipsoidal shape. Concurrently, in each lamella, chain tilt and slip are likely to occur under shearing. The effect of such deformation is to align the chains more nearly parallel to the tensile axis.

On further stretching, blocks of crystals, attached by tie molecules, are pulled out of the lamellae. This phenomenon gradually destroys the microvoid network, created at earlier stages of deformation. As a result, scattering due to density fluctuation decreases. Thus, during stretching of individual spherulites, it was observed that the equatorial region appeared to be less dark for a longitudinal strain, ϵ_L close to 0.8, and that, for much larger strains, the dark band completely disappeared.
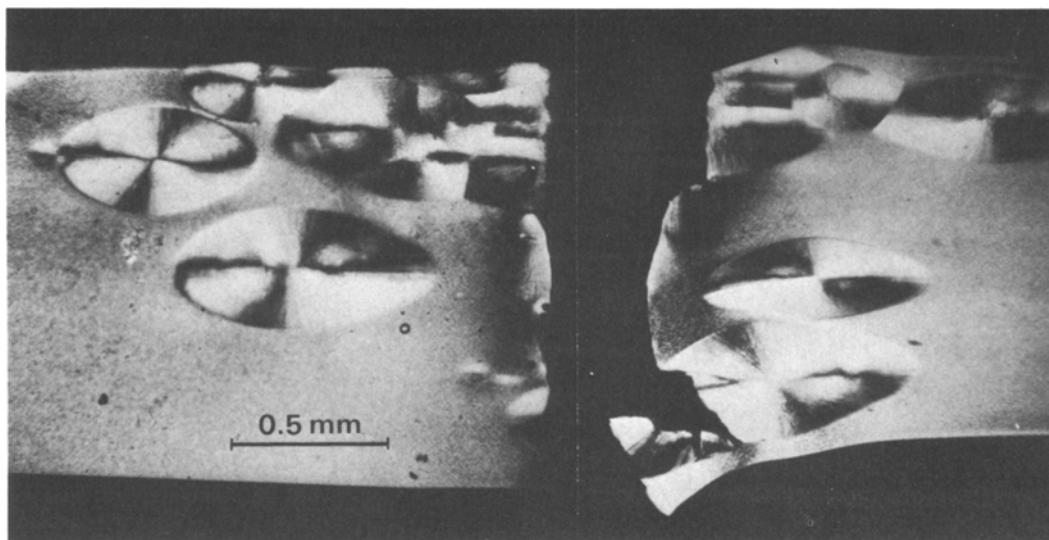
Figure 13 Fracture of the composite sample observed in Fig. 11. Note the brittleness of the spherulites.

On the other hand, in the polar regions, the crystalline lamellae are parallel to the draw direction and their deformation can be compared to the stretching of single crystals on a substrate. According to the model proposed by Peterlin [34—37], chain tilt and slip leads to the break up of lamellae into smaller folded chain blocks, separated by cracks. The cracks are bridged by many microfibrils pulled out of the lamellae. In such a mechanism, chains, which were tangential, tend to align preferentially in the radial draw direction. Accordingly, the initial negative bi-refringence becomes first zero (observation of a dark line between polarizers at $\pm 45°$) and then more and more positive (observation of a coloured line).

4.3. Correlation between macroscopic mechanical behaviour and microstructure observation

It was observed that strains reached in the *in situ* deformation of homogeneous films were in agreement with those measured with the Instron machine. However, stresses were somewhat lower in *in situ* deformation, probably because of the experimental procedure. Films used for *in situ* experiments were very thin (for instance $40 \mu m$ for Sample 6) with respect to the spherulite diameter ($160 \mu m$ in Sample 6); they were strained step-by-step, which induced some stress relaxation at each step.

On the other hand, tensile tests of composite Samples 7 and 8, cannot be directly compared with those of homogeneous samples. The determination of ϵ_L and ϵ_T allowed us to simply associate the total deformation of a single spherulite in an homogeneous matrix with the evolution of its microstructure.

Nevertheless, taking into account the above remarks, it was possible to propose some interpretation of the mechanical behaviour of polybutene, from the comparison of mechanical property data with microstructure observations. It has been seen in Section 3.1. that specimens crystallized at a high temperature exhibited a very specific mechanical behaviour with respect to samples crystallized at lower temperatures or by quenching. A change in the crystallization temperature T_c usually has several effects on the crystalline morphology. When T_c increases, the crystalline fraction and the spherulite diameter increase (cf. Fig. 3). The crystalline lamellae are expected to be thicker and less twisted. It can be inferred from *in situ* observations that such a morphological evolution will promote interlamellar separation during straining and that this separation mechanism is mainly responsible for some specific mechanical properties, higher elastic modulus, homogeneous macroscopic deformation and high recovery from large extensions. These properties have been examined in detail for the so-called "hard elastic" fibres and films [31, 32, 38]. In our case, the hard elastic properties principally involve the equatorial regions of the spherulites, which can be taken as parts of a hard elastic film, and also, to a lesser

degree, the diagonal regions. Because of early brittle ruptures, the high recovery from large extensions was principally observed for *in situ* experiments performed on individual spherulites embedded in a microspherulitic matrix. As long as the dark band was observed within the spherulites, the elastic longitudinal strain ϵ_{el} was found to be more important than the permanent plastic strain ϵ_{pl}. The plastic strain became larger than the elastic one, only when the dark band began to disappear. This was obtained in our experiments for a total longitudinal strain close to 0.8.

Concerning the rupture mechanism, microvoids between separated and bent crystalline lamellae can be considered as microcracks which favour early brittle intraspherulitic fracture. It was actually observed in our experiments that the fracture line followed spherulite radii. This rupture may have been initiated in regions with high stress concentrations. According to different authors, these regions may be either the spherulite boundaries [3, 5] or the spherulite core [8].

On the other hand, low-temperature crystallization leads to small and less crystalline spherulites, in which lamellae are thinner and much more twisted. As a result, the hard elastic character is less pronounced, because, as in polyethylene, the deformation mechanism rapidly involves some irreversible chain slip within the crystalline lamellae.

It would be interesting, but rather difficult, to separate the respective effects of the main morphological parameters (degree of crystallinity, spherulite size, lamellae thickness etc.). For instance, it is known that, for a given spherulite size, crystallinity and lamella thickness can be increased by annealing [39, 40]. A complementary experiment was performed with Sample 2, crystallized in iced water. It was annealed for 90 min at 70° C, and then tested on the Instron machine. The general shape of the stress–strain curve for the annealed sample was identical to the one for Sample 2, but it appeared that annealing slightly improved the strength and the modulus. Such an experiment confirms that crystallinity and lamella thickness have an influence on the reinforcement of the material, independent of the influence of the spherulite size.

5. Summary and conclusions

Thin tensile specimens of polybutene-1 (Modification I) were tested with a variety of spherulitic morphologies. It was shown that their stress–strain behaviour was the one of a hard elastic material whose modulus and strength are increasing functions of the spherulite size and the degree of crystallinity. However the specimens exhibit an increasing intraspherulitic brittleness as their strength is improved.

Specimens with large spherulites embedded in a microspherulitic ductile matrix were investigated *in situ* by optical microscopy while deformed in tension. It was shown that the bending and separation of the crystalline lamellae situated in the equatorial regions of the spherulites play a major role in the large elastic recovery. The plastic glide of the lamellae parallel to the diagonal radii are supposed to be more important for increasing stresses. While this process becomes prominent, the elastic separation between the equatorial lamellae is observed to be relaxed, as shown by the disappearance of the dark band phenomenon associated with this lamellar separation.

References

1. H. D. KEITH and F. J. PADDEN Jr, *J. Polymer Sci.* **41** (1959) 525.
2. P. H. GEIL, "Polymer Single Crystals" (Interscience, New York, 1963) p. 427.
3. I. L. HAY and A. KELLER, *Kolloïd-Z* **204** (1965) 43.
4. V. A. KARGIN and I. Yu. TSAREVSKAYA, *Polymer Sci. USSR* **8** (1966) 1601.
5. V. A. KARGIN, G. P. ANDRIANOVA and G. G. KARDASH, *ibid.* **9** (1967) 289.
6. R. YANG and R. S. STEIN, *J. Polymer Sci. A–2* **5** (1967) 939.
7. R. G. CRYSTAL and D. HANSEN, *ibid.* **6** (1968) 981.
8. T. W. HAAS and P. H. MAC RAE, Society of Plastics Engineers 27th Annual Technical Meeting, New York, May 1979 (Society of Plastics Engineers, Chicago, 1969) p. 16.
9. J. L. WAY and J. R. ATKINSON, *J. Mater. Sci.* **6** (1971) 102.
10. P. ALLAN and M. BEVIS, *Phil. Mag.* **35** (1977) 405.
11. K. SASAGURI, S. HOSHINO and R. S. STEIN, *J. Appl. Phys.* **35** (1964) 47.
12. K. SASAGURI, R. YAMADA and R. S. STEIN, *ibid.* **35** (1964) 3188.
13. G. NATTA, P. CORRADINI and I. W. BASSI, *Nuovo Cimento Suppl.* **15** (1960) 52.
14. V. PETRACCONE, B. PIROZZI, A. FRASCI and P. CORRADINI, *Eur. Polymer J.* **12** (1976) 323.
15. C. COJAZZI, V. MALTA, G. CELOTTI and R. ZANNETTI, *Makromol. Chem.* **177** (1976) 915.
16. V. F. HOLLAND and R. L. MILLER, *J. Appl. Phys.* **35** (1964) 3241.
17. J. BOOR Jr and J. C. MITCHELL, *J. Polymer Sci. A* **1** (1963) 59.

18. B. H. CLAMPITT and R. H. HUGHES, *J. Polymer Sci. C* 6 (1964) 43.
19. R. ZANETTI, P. MANARESI and G. C. BUZZONI, *Chim. Ind. (Milan)* 43 (1961) 735.
20. S. Y. CHOI, J. P. RAKUS and J. L. O'TOOLE, *Polymer Eng. Sci.* 6 (1966) 349.
21. C. D. ARMENIADES and E. BAER, *J. Macromol. Sci. Phys.* B1 (2) (1967) 309.
22. R. S. STEIN and M. B. RHODES, *J. Appl. Phys.* 31 (1960) 1873.
23. G. PICOT, R. S. STEIN, M. MOTEGI and H. KAWAI, *J. Polymer Sci. A−2* 8 (1970) 2115.
24. G. MEINEL and A. PETERLIN, *J. Polymer Sci. A−2* 9 (1971) 67.
25. R. J. SAMUELS in "Plastic Deformation of Polymers" edited by A. Peterlin (Marcel Dekker, New York, 1971) p. 241.
26. C. G'SELL and J. J. JONAS, *J. Mater. Sci.* 14 (1979) 583.
27. R. J. SAMUELS, *J. Polymer Sci. C* 13 (1966) 37.
28. E. WEYNANT and J. M. HAUDIN, unpublished results.
29. T. T. WANG, *J. Polymer Sci (Polymer Phys. Ed.)* 12 (1974) 145.
30. P. DEBYE and A. M. BUECHE, *J. Appl. Phys.* 20 (1949) 518.
31. R. G. QUYNN and H. BRODY, *J. Macromol. Sci. Phys.* B5 (4) (1971) 721.
32. T. HASHIMOTO, K. NAGATOSHI, A. TODO and H. KAWAI, *Polymer* 17 (1976) 1063 and 1075.
33. T. HASHIMOTO, A. TODO, Y. MURAKAMI and H. KAWAI, *J. Polymer Sci.* (Polymer Phys. Ed.) 15 (1977) 501.
34. P. INGRAM, H. KIHO and A. PETERLIN, *J. Polymer Sci. C* 16 (1967) 1857.
35. A. PETERLIN, *Kolloid Z.Z. Polymere* 233 (1969) 857.
36. *Idem, J. Mater. Sci.* 6 (1971) 490.
37. *Idem, Polymer Eng. Sci.* 17 (1977) 183.
38. E. S. CLARK in "Structure and Properties of Polymer Films", edited by R. W. Lenz and R. S. Stein (Plenum Press, New York, 1973) p. 267.
39. E. W. FISCHER and G. F. SCHMIDT, *Angew. Chem.* 74 (1962) 511.
40. S. KAVESH and J. M. SCHULTZ, *J. Polymer Sci. A−2* 9 (1971) 85.